ENVIRONMENTAL RESEARCH
CLIMATE

PAPER • OPEN ACCESS

Global warming level indicators of climate change and hotspots of exposure

To cite this article: Michaela Werning *et al* 2024 *Environ. Res.: Climate* **3** 045015

IOP Publishing Environ. Res.: Climate 3 (2024) 045015 https://doi.org/10.1088/2752-5295/ad8300

ENVIRONMENTAL RESEARCH
CLIMATE

CrossMark

OPEN ACCESS

RECEIVED
17 May 2024

REVISED
20 September 2024

ACCEPTED FOR PUBLICATION
3 October 2024

PUBLISHED
23 October 2024

PAPER

Global warming level indicators of climate change and hotspots of exposure

Michaela Werning[1,*], Daniel Hooke[2], Volker Krey[1], Keywan Riahi[1], Bas van Ruijven[1] and Edward A Byers[1]

[1] Energy, Climate & Environment Program, International Institute of Applied Systems Analysis, Schlossplatz 1, 2361 Laxenburg, Austria
[2] Met Office Hadley Centre, Exeter, United Kingdom
[*] Author to whom any correspondence should be addressed.

E-mail: werning@iiasa.ac.at

Keywords: climate change, climate change impacts, hazards, ISIMIP, exposure

Supplementary material for this article is available online

Abstract

In the 21st century, a growing population will be exposed to various hazards caused by a warming climate. Here we present a new database of 12 climate change indicators with a total of 42 variants at different global warming levels (GWLs) (1.2 °C–3.5 °C), which is based on global climate and hydrological model data from the Coupled Model Intercomparison Project round 6 and the Inter-Sectoral Impact Model Intercomparison Project round 3b at 0.5° spatial resolution. It comprises of indicators relating to temperature and precipitation extremes, heatwave events, and hydrological variability. To facilitate the comparison of hazards from different indicators, including for an audience without a scientific background, we have developed a bivariate hazard score which is applied on the grid cell level and incorporates statistics on both the absolute hazard (e.g. low or high precipitation) and the relative change under global warming compared to the reference period (e.g. a large change from low to high precipitation). Additionally, we calculate exposed land area and population through the 21st century for a large set of countries and regions by combining this score with gridded projections of population from the Shared Socioeconomic Pathways (SSPs). The datasets are intended for use by the wider research community and analysts seeking digestible climate hazard and exposure data summarized by GWLs. To illustrate potential uses of the data, in a preliminary analysis we find that even at 1.5 °C large parts of the land area and population face substantial unavoidable risks from multiple indicators, with 86% of the world's population exposed to at least three indicators with at least medium hazard using the population projections for SSP2 in the year 2050. This picture only worsens with increasing warming, as the land areas facing the highest number of impacts coincide with some of the most densely populated parts of the world.

1. Introduction

Growing interest and concern about climate change and associated data products is driving increased research and analysis on the topic; not just from climatologists, but also across many sectors of research, business, and industry. The interest stems from the need to understand not just the biophysical changes as reported by the field of climate and earth systems science, but ultimately the associated societal risks. To conceptualize the climate risk, as it is defined in a Special Report by the Intergovernmental Panel on Climate Change (IPCC) (Field *et al* 2012), it is essential to understand the entire risk chain, i.e. how biophysical changes become hazards, who and what is exposed to these hazards, and what is the vulnerability of those exposed.

Despite advances in cloud computing and open datasets, working with global climate model (GCM) data outputs remains by and large a niche activity, given the dataset sizes, programming skills, and computational requirements to work with it, let alone the climate domain knowledge. To meet the growing interest, accelerate our understanding, and communicate the urgency of the climate crisis, an increasing number of indicator datasets, composed of post-processed climate model output in more digestible sizes and variables, are being produced and presented in online platforms (e.g. Global Hotspots Explorer (IIASA 2019); Climate Change Knowledge Portal (World Bank 2021); Climate Impacts Explorer (Climate Analytics 2022); European Climate Data Explorer (EEA 2022); IPCC AR6-WGI Atlas (IPCC 2022c); ISIpedia (ISIMIP 2022)). The aim behind this work is to publicly provide more accessible climate data products, which have been calculated consistently, for the use by other researchers, analysts, practitioners, and the general public.

A major contributor to the field has been the Inter-Sectoral Impact Model Intercomparison Project (ISIMIP), which coordinates activities involving climate impact models, such as global hydrological, crop growth, wildfire, fisheries, and energy sector models, amongst others, to enable model intercomparison and elucidation of key impact uncertainties under different climatic and socioeconomic scenarios. To facilitate this, the framework uses consistently bias-corrected and downscaled climate model forcing data (to 0.5° grid resolution) from a 5-member ensemble that was chosen to cover the Coupled Model Intercomparison Project round 6 (CMIP6) range of temperature and precipitation uncertainty (Frieler *et al* 2024a). The high resolution, spatio-temporal consistency, and accessibility of the ISIMIP forcing data and subsequent impact model projections has made it the most successful high-impact initiative in climate impacts research in the past decade.

A large number of previous assessments have worked to evaluate a range of climate impacts using similarly consistent approaches, with the aim of highlighting the multi-faceted challenges faced under a warming climate. Of prominence, these studies using ISIMIP data have largely pioneered the assessment of climate impacts at global warming levels (GWLs) (e.g. +1.5 °C, 2.0 °C, 3.0 °C above pre-industrial temperatures), with not only direct relevance to policymakers but also increased accessibility of the findings to the general public. For example, several multi-impact studies (Piontek *et al* 2014, Schleussner *et al* 2016, Frieler *et al* 2017, Byers *et al* 2018) assessing the impacts between 1.5 °C and 2.0 °C, provided substantial evidence to the IPCC Special Report on Global Warming at 1.5 °C, by including consistent indicators on a combination of, for example, temperature and precipitation extremes, hydrology, crop yields, sea level rise, coral reef impacts, energy demands, ecosystems, malaria, cyclones, floods, wildfire, drought, and variability of river discharge. Such multi-impact assessments have added huge value to downstream users, although comparability across indicators can be a challenge. More recent assessments have used more sophisticated extreme event impact models (tropical cyclones, crop failure, wildfires, droughts, and heatwaves) (Lange *et al* 2020) and have subsequently evaluated the inter-generational inequities by calculating lifetime exposure across age cohorts (Thiery *et al* 2021).

Prior work has translated changes in multiple hazards to comparable indices and metrics (Giorgi 2006, Diffenbaugh *et al* 2007, Diffenbaugh and Giorgi 2012, Piontek *et al* 2014, Byers *et al* 2018, Sun *et al* 2019, Rising *et al* 2022), with the aim of helping communicate the severity of changes of different climatic variables and indicators. It can require the definition of subjectively informed (Giorgi 2006) or statistically derived (Williams *et al* 2007) thresholds upon which to base scoring, but enables non-experts to make relative comparisons both within and across indicators for given locations or warming levels. This is crucial as a climate hazard's impact can vary by its absolute or relative change, and often both. For instance, the significance of tropical nights doubling annually differs greatly between areas with 60 versus five such nights.

Here we present a collection of consistent gridded datasets of climate hazard indicators by six policy-relevant GWLs, provided in (i) absolute units, (ii) relative changes in percentages, and (iii) a comparable hazard score that uses a bivariate approach to account for both relative changes and changes in the absolute values. We test and demonstrate this across 12 indicators (with 42 variants), covering precipitation, heat-related extremes, and hydrology, that are primarily derived from the latest round of the ISIMIP project (3b). We subsequently use these indicators to calculate land and population-weighted exposure using projections from the Shared Socioeconomic Pathways (SSPs) at national and regional scales to demonstrate potential applications of the data for further climate impacts assessment. To communicate these risks of climate change to a wider public, the resulting global maps at a high spatial resolution of $0.5° \times 0.5°$ are hosted online (www.climate-solutions-explorer.eu) and presented alongside national dashboards presenting information on avoided impacts by mitigating to 1.5 °C.

2. Methods

2.1. Overview

Using data from different GCMs forced by Representative Concentration Pathways (RCPs), as well as data from global hydrology models (GHMs), we calculate 12 hazard indicators (e.g. cooling degree days) with a total of 42 variants (e.g. cooling degree days using different set-point temperatures) to investigate the change of these indicators at different GWLs. Hazards are assessed at 1.2 °C, the approximate current level of global

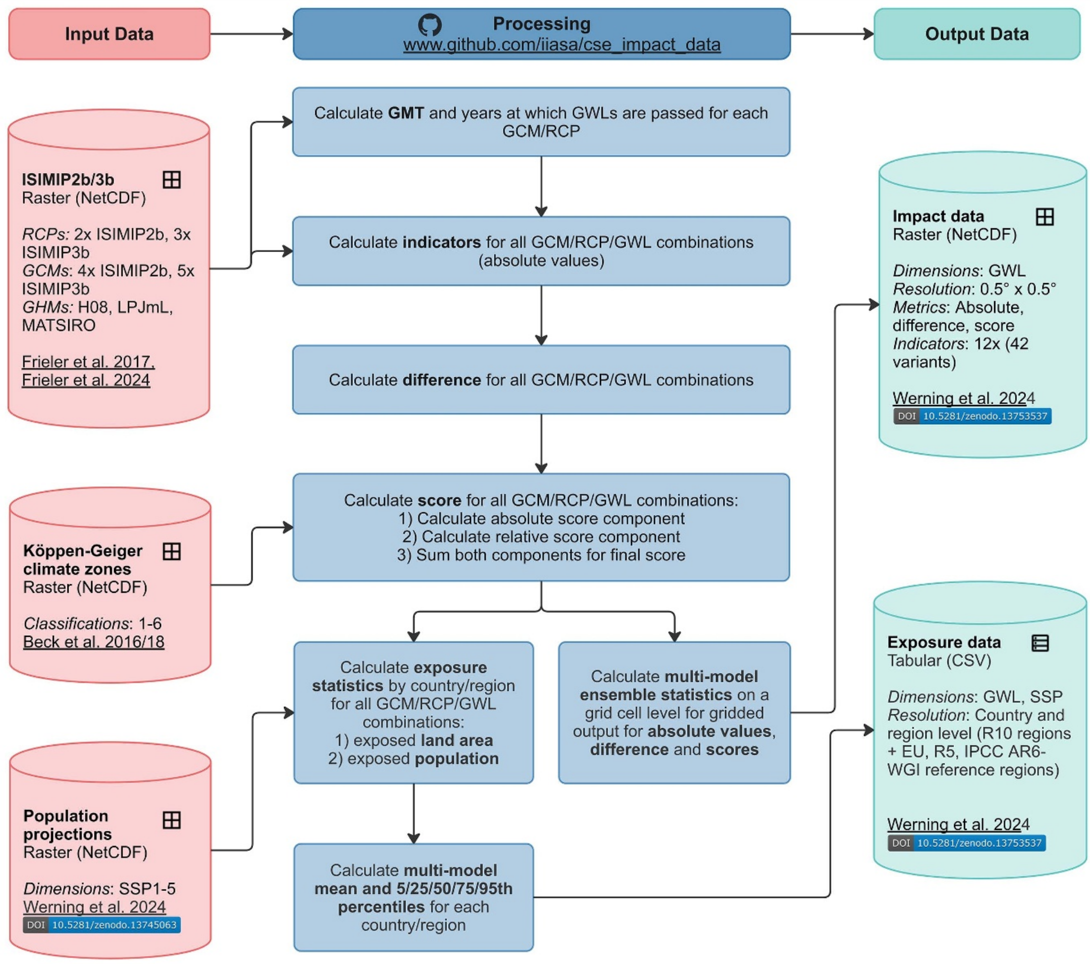

Figure 1. Overview of the entire workflow. The red column on the left shows the input data that were used during the calculation of the indicators and output datasets. The different stages of the calculation are listed in blue in the middle column and the generated output datasets are shown in green on the right.

mean temperature (GMT) change compared to a pre-industrial period average (Forster *et al* 2024), as well as at 1.5 °C, 2.0 °C, 2.5 °C, 3.0 °C, and 3.5 °C, using multi-model ensemble statistics. To facilitate comparison with recent conditions, we calculate the difference between the different levels of global warming and our chosen reference period, which covers the years 1974–2004. We then map every indicator to a common hazard score to help compare changes in the hazard of different indicators, advancing methods used in previous work (Byers *et al* 2018) by simultaneously accounting for both the existing level of each hazard and the additional change caused by global warming. Exposure to hazards above certain thresholds is also calculated using land area maps and gridded population projections from the SSPs. A schematic overview of the workflow is shown in figure 1.

2.2. Climate forcing and impact model data

Data from ISIMIP are used to calculate the indicators, primarily from the ISIMIP input forcing data and a selection of GHMs. ISIMIP offers a framework for consistently modelling the cross-sectoral and cross-scale impacts of climate change by providing a common modelling protocol and a common set of climate forcing and other input datasets which are made available to the scientific community in a central archive (http://data.isimip.org). Sectors included are, amongst others: water, agriculture, energy supply and demand, forests, and coastal systems. ISIMIP also provides a multi-centennial pre-industrial reference simulation to isolate historical warming effects from other drivers and identify the pure climate change signal (Frieler *et al* 2017, 2024a, 2024b).

Precipitation and temperature indicators are calculated using data from the latest ISIMIP simulation round 3b, which is based on CMIP6 global climate and earth systems models (Lange and Büchner 2021). For the hydrology indicators, which required data that were not yet available from simulation round 3b at the time of calculation, data from simulation round 2b are used (Lange and Büchner 2017, Gosling *et al* 2023). ISIMIP2b is based on CMIP5 and—although not from the latest CMIP round—is still the most recent

Table 1. Overview of primary models and experiments available in ISIMIP simulation rounds 2b and 3b, as used in this study.

Simulation round	Based on data from	Global climate models	Experiments
ISIMIP2b	CMIP5	GFDL-ESM2M, HadGem2-ES, IPSL-CM5A-LR, MIROC5	piControl, historical, future (rcp26, rcp60)
ISIMIP3b	CMIP6	GFDL-ESM4, IPSL-CM6A-LR, MPI-ESM1-2-HR, MRI-ESM2-0, UKESM1-0-LL	piControl, historical, future (ssp126, ssp370, ssp585)

complete set of ISIMIP hydrology data available. Once ISIMIP have released data from more GHMs in simulation round 3b, the hydrology indicators will be updated accordingly. In the meantime, care should be taken when using the data for analysis based on a GWL of 3.5 °C as the hydrology indicators are not available for this GWL due to the limited range of RCPs in ISIMIP2b (table 2, SI). The ISIMIP data are provided at daily temporal and 0.5° spatial resolution and have been statistically downscaled and adjusted to correct biases between the data simulated by the GCMs and an observation-based reference while still preserving indicator trends (Frieler *et al* 2017, 2024b, Lange 2019, 2021). Primary climate forcing datasets in ISIMIP were selected from the entire CMIP ensemble based on process representation, structural independence, and climate sensitivity (amongst other factors) (Lange 2021), and are intended to largely cover the range of uncertainty across temperature and precipitation (table 1).

2.3. GMT calculation

To assess the climate change hazard, we follow the established time-sampling approach (Piontek *et al* 2014, Schleussner *et al* 2016, James *et al* 2017, Schurer *et al* 2017) of selecting a 31-year temperature time slice, centred on the year at which each GCM/RCP combination passes six different levels of GMT change: 1.2 °C, 1.5 °C, 2.0 °C, 2.5 °C, 3.0 °C, and 3.5 °C (SI section 1).

In line with the ISIMIP temperature protocols (ISIMIP3b temperature thresholds and time slices, 2024), the change in GMT is deduced using the entire time period covered by the pre-industrial control runs (i.e. 1601–2100 for ISIMIP3b data and 1661–2099 for ISIMIP2b data, respectively). We note that more recent studies have used 1850–1900 to represent pre-industrial conditions in line with recent IPCC assessment reports (Allen *et al* 2018), although this has caveats, too (James *et al* 2017, Schurer *et al* 2017).

2.4. Socioeconomic pathways

The climate change indicators are combined with spatial population projections from SSPs 1–5, based on Jones and O'Neill (2016) and Kc and Lutz (2017), and scaled to match the latest available projections (KC *et al* 2024) (SI section 3). The SSPs form a framework that the climate change research community has co-developed and adopted to facilitate the integrated analysis of future climate hazards, vulnerabilities, adaptation, and mitigation. The SSPs span five narrative storylines about socioeconomic development (O'Neill *et al* 2017), and include quantitative driver projections of population, gross domestic product, and urbanization amongst other indicators (Riahi *et al* 2017).

2.5. Indicator calculation

2.5.1. Overview of indicators

In total, a set of 12 indicators from three different categories are assessed (table 2). Indicators are calculated for the six different GWLs and all combinations of available GCMs and RCPs (tables SI 1 and 2). For the hydrology indicators, we use data from three of the available GHMs in ISIMIP2b (H08 (Hanasaki *et al* 2018), LPJmL (von Bloh *et al* 2018), MATSIRO (Takata *et al* 2003)), which enlarges the set of available combinations. Additionally, indicators are also calculated for our chosen reference period spanning the years 1974–2004, which is used as a baseline to evaluate the change in climate hazards for the different GWLs. If the 31-year period for a GWL overlaps the start of the future projections (<2005 for ISIMIP2b and <2015 for ISIMIP3b), the historical ISIMIP datasets are used to fill the entire 31-year period.

Most of the precipitation and temperature indicators are based on definitions developed by the World Climate Research Program Expert Team on Climate Change Detection and Indices (Klein Tank *et al* 2009) to allow individuals, countries, and regions to calculate the change in frequency or severity of extreme climate events in a consistent way.

2.5.2. Multi-model ensemble statistics

The calculation of each indicator provides us with a subset of data for each GWL, defined by the GCM, RCP, and—in the case of the hydrology indicators—also the GHM. For all ensemble members in these subsets, the

Table 2. Overview of climate hazard indicators. Number of variants refers to the sub-indicators that have been calculated, for example, in heatwave events the combinations of different percentile thresholds and event durations. Additional indicator information is provided in SI section 2 and table SI 3.

Indicator	Variants	Description and calculation	Indicator units	Methodological reference
		Precipitation		
(Very) Heavy precipitation days	2	Annual number of days with ⩾(20) 10 mm daily precipitation	days yr^{-1}	(Klein Tank *et al* 2009)
(Very) Wet days	2	Annual sum of the daily precipitation amount on wet days (daily precipitation ⩾1.0 mm) with a precipitation amount larger than the (99th) 95th percentile of precipitation on wet days in the reference period	mm yr^{-1}	(Klein Tank *et al* 2009)
Precipitation intensity index	1	Annual total precipitation amount divided by the annual number of wet days with a precipitation amount ⩾1 mm	—	(Klein Tank *et al* 2009)
Consecutive dry days	1	Maximum number of consecutive dry days for days with a daily precipitation amount <1 mm	days yr^{-1}	(Klein Tank *et al* 2009)
		Hydrology and water resources		
Drought intensity	2	The proportion between daily volume deficit of runoff (qtot) or discharge (dis) (m^3 s^{-1}) below the 10th percentile daily discharge (Q_{90}) and drought event duration (days)	—	(Wanders and Wada 2015)
Seasonality	2	The coefficient of variation (standard deviation divided by the mean) of mean monthly discharge (dis) or runoff (qtot). Lower values (<1) represent low seasonality (i.e. flows do not vary much through the year). Higher values indicate that the seasonal water availability is becoming more unpredictable.	—	(Byers *et al* 2018)
Inter-annual variability	2	The coefficient of variation (standard deviation divided by the mean) of mean annual discharge (dis) or runoff (qtot). Lower values (<0.5) represent low inter-annual variability (i.e. annual flows do not vary much between years). Higher values indicate that the annual water availability is becoming more unpredictable.	—	(Byers *et al* 2018)
Water stress index	1	Fraction of net human demands (domestic, industrial, irrigation) divided by renewable surface water availability, also known as the withdrawal to availability ratio. High water stress means that a high proportion of the available water is being used.	—	(Raskin 1997, Burek *et al*, 2016, Satoh *et al* 2017)
		Temperature		
Heatwave events	12	The annual number of heatwave events lasting 3/5/7/10 or more consecutive days above the historical 95/97/99th percentile daily mean wet bulb air temperature	events yr^{-1}	(Byers *et al* 2018)
Heatwave days	12	The annual sum of days from heat stress events lasting 3/5/7/10 or more consecutive days above the historical 95/97/99th percentile daily mean wet bulb air temperature	days yr^{-1}	(Byers *et al* 2018)
Consecutive tropical nights	1	The maximum number of consecutive days where the daily minimum air temperature does not fall below 20 °C	days yr^{-1}	Based on (Klein Tank *et al* 2009)
Cooling degree days	4	The absolute number of cooling degree days above a 26 °C/24 °C/20 °C/18.3 °C set-point temperature for the daily mean air temperature	degree days yr^{-1}	(Byers *et al* 2018)

relative difference to the reference period and the hazard score are calculated. In the next step, multi-model ensemble statistics are generated at the grid cell level for each subset and each indicator at the six GWLs. Since not all GCM/RCP/(GHM) combinations reach all GWLs due to the differing climate sensitivity of the GCMs, the number of combinations making up the subsets and therefore contributing to the ensemble statistics differs for each GWL (tables SI 1 and 2), i.e. the number of combinations contributing at 3.0 °C is smaller than at 1.5 °C.

2.5.3. Score conversion

To facilitate the comparison of different indicators, we have developed a bivariate hazard score. This continuous bivariate hazard score ranges from no hazard (with a score of 0) to a very high hazard (with a score of 6) and is applied to every grid cell. The motivation for this new bivariate approach is to include both the change in the absolute value of the indicator as well as the relative change in distribution compared to the reference period. For example, locations that already have a high value for an indicator (e.g. water stress or heatwave events), may only experience small relative changes because the situation is already severe. Conversely, locations with comparatively benign conditions may experience relatively high changes. Our bivariate approach consists of two steps.

In the first step, the absolute change in the indicator value is assessed and given a continuous score between 0 (no hazard) and 3 (very high hazard). The basis for this assessment is the reference period, as we consider this to be a representation of conditions without considerable influence of climate change. To map the value in every grid cell to a score between 0 and 3, the 50th, 75th, and 95th percentile of the data in the reference period are used, with the 50th, 75th, and 95th percentile being the thresholds for a score of 1, 2, and 3, respectively. This puts the conditions in every grid cell in relation to the overall global distribution of values for the reference period. A grid cell at 2 °C of GMT change with an indicator value that is larger than the 95th percentile of the data for the reference period is assigned a score of 3, for example (first row in figure 2). This component therefore captures the absolute value of the indicator.

In the second step, the change in the indicator value on a local level is captured. For this, we assess the change of indicator value in every grid cell and relate it to the initial distribution of values for that grid cell in the reference period. The starting point for this assessment is the distribution of the 31 annual values spanning the reference period, for which the standard deviation is calculated. To assign a score to every grid cell, the value for the reference period is subtracted from the value at each GWL and then divided by the standard deviation for every grid cell. The resulting values are then mapped to a continuous score between 0 and 3, with 1, 2, and 3 as the threshold for a score of 1, 2, and 3, respectively, thereby indicating how much the value has shifted in terms of the standard deviation of the original distribution in the reference period. A grid cell at 2.0 °C of GMT which shows a difference to the reference period that is larger than two standard deviations is therefore assigned a score larger than 2, which amounts to at least medium hazard (second row in figure 2).

Finally, the scores from step one and two are summed to create the final impact score ranging from 0 to 6 (last row in figure 2). The score conversion methodology described above is applicable to all indicators, although the following refinements were made for setting the absolute thresholds for the heatwave and hydrology indicators:

- **Heatwaves**: Wet bulb temperatures of 18 °C, 25 °C, and 30 °C are used as the thresholds for a score of 1, 2, and 3, respectively, instead of the 50th, 75th and 95th percentiles of the reference period, as the combined measurement of heat and humidity is a good indication of the risk posed to humans.
- **Water stress index**: Absolute values of water stress independent of the data are used as thresholds in the score conversion, with 0.1, 0.2, 0.3, and 0.4 mapping to a score of 0, 1, 2, and 3 respectively as it is commonly agreed that an index of 0.2–0.4 represents water stress (Raskin 1997).
- **Seasonality and inter-annual variability**: The percentiles used to map the absolute values at the GWLs are calculated for each Köppen–Geiger climate zone (Beck *et al* 2018) separately to take into account different land, climate, and water-cycle characteristics.

Another challenge when designing a hazard score is how to assess the hazard for locations that change from not being exposed to any hazard at all in the reference period to being exposed to some hazard (small or large) in the future. As the standard deviation for the reference period is zero in this case, the second component of the score cannot be calculated. To assign a score to grid cells which show this behaviour, the data are assigned a score solely based on the first step as described above, which allows to at least capture part of the change. For the majority of indicators, this occurs in <3% of grid cells, whilst for 'Tropical nights' it

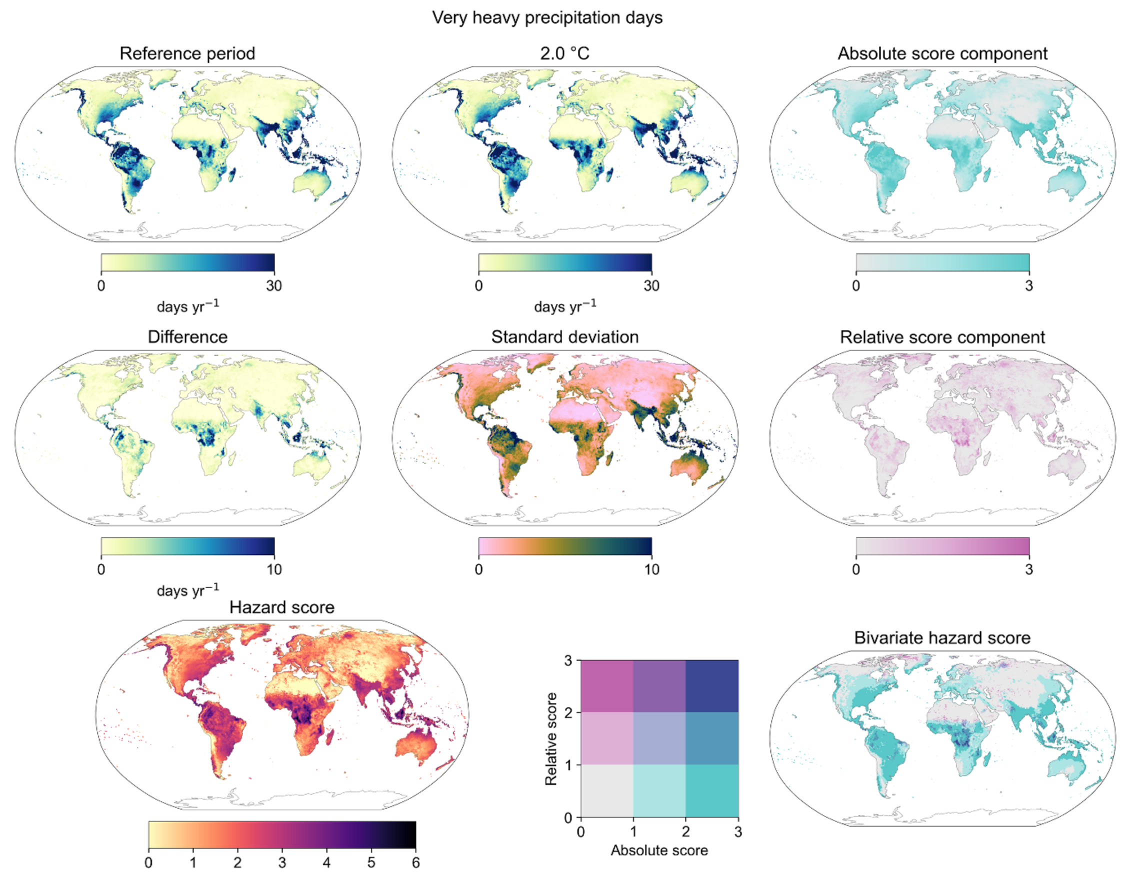

Figure 2. Score methodology process illustrated for one ensemble member (MPI-ESM1-2-HR, SSP370) of the indicator 'Very heavy precipitation days'. The first row shows the indicator values for the reference period (1974–2004) on the left, the indicator values for a global warming level of 2.0 °C in the middle, and the conversion of the absolute score component on the right, which shows high score values in places that coincide with high absolute indicator values. The absolute difference between the reference period and 2.0 °C, as well as the standard deviation of the reference period, and the resulting relative score component are shown in the second row (from left to right). The bottom row shows the combination of the absolute and relative score component, both as the resulting score on the left and in a bivariate plot on the right to highlight the contributions of the two components to the final score. The highest scores can be found in places that already start with a high number of very heavy precipitation days and additionally experience a large change between the reference period and the future global warming level. Areas with a strong relative change but an overall small number of very heavy precipitation days per year, on the other hand, result in a low to medium score value.

was 12% at 2.0 °C, as a number of mid-latitude locations start having tropical nights when they previously had none.

Results for the indicator 'Very heavy precipitation days' are shown in figure 3 with the scores for all GWLs on the right, together with the indicator value and the relative change to the reference period in the left and middle column, respectively. As expected, the relative difference between the reference period and the GWLs increases with increasing GMT, as do the hazard scores. Especially the northern latitudes, Greenland and the deserts show a change of more than 100% compared to the reference period for the higher GWLs. Even though the percentage-wise change is large, the actual number of very heavy precipitation days in these areas is still very low, which is captured by the score value, resulting in a low to medium hazard score in these regions. When looking at northern Africa, areas with missing values in the difference plots can be noted. This is due to the precipitation amount in those grid cells changing from zero in the reference period to non-zero for the GWLs, hence a difference in percentages cannot be calculated. Therefore, only the absolute component is scored which results in no hazard for these regions, as the indicator values are still very small compared to the rest of the world.

Temperature based indicators, such as 'Heatwave events' or 'Tropical nights', show comparatively higher scores than the precipitation- or hydrology- based ones (figure 4). This observation is consistent across all GWLs (figures SI 1–3) and can be attributed to the bigger change in air temperature with increasing GMT compared to the reference period and compared to other climatic input variables.

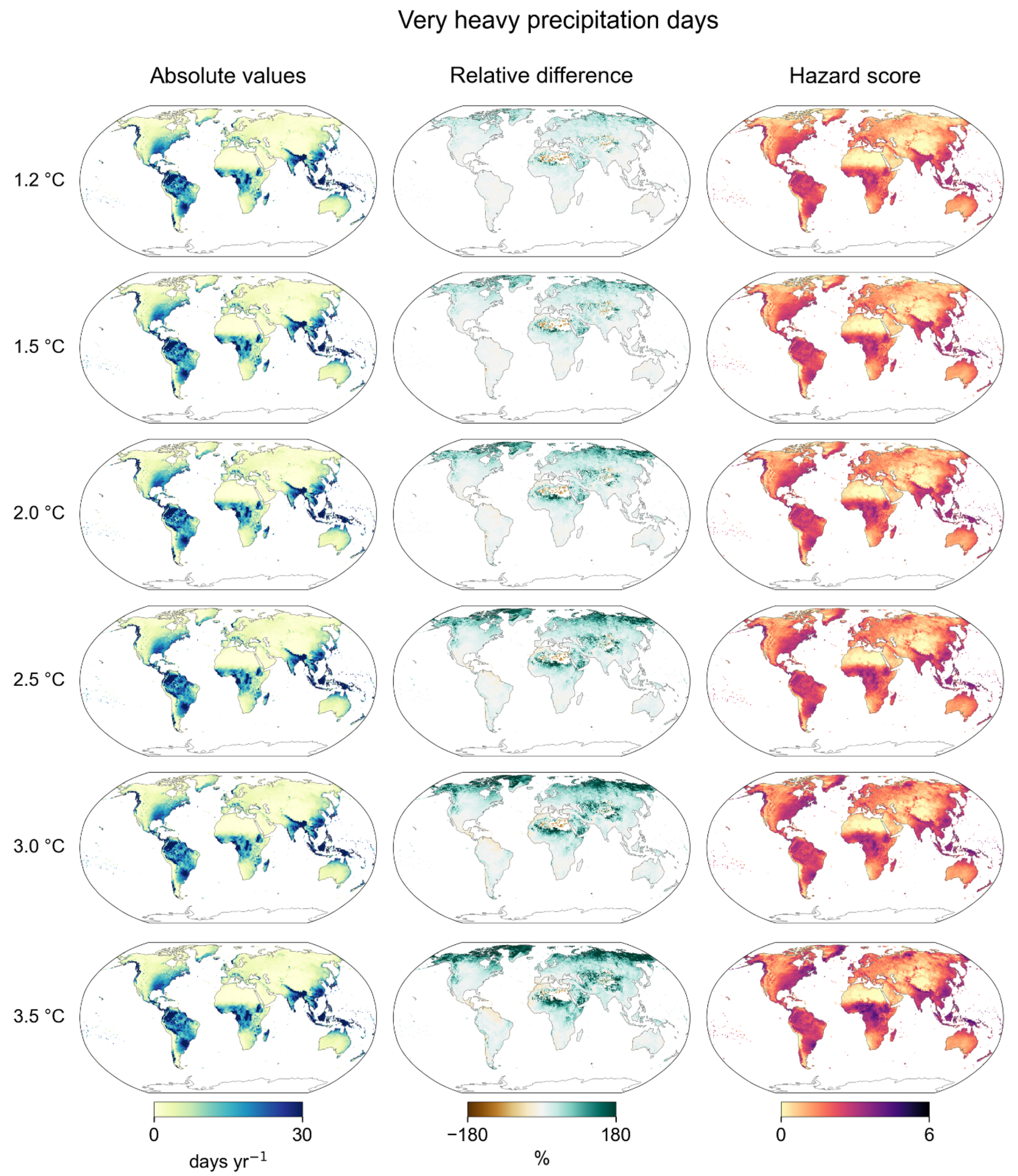

Figure 3. Absolute values, relative differences, and scores for all global warming levels and the indicator 'Very heavy precipitation days'. Shown in the left column is the multi-model median for each global warming level. The middle column shows the multi-model median of the relative difference between the global warming level and the reference period (1974–2004). The hazard score (multi-model median) for each global warming level is shown on the right.

2.6. Exposure calculation

After the conversion to hazard scores, the indicator hazard data can be combined with other spatial datasets to assess exposure. Here this is done for land area, which is static through time, and also gridded population projections for SSPs 1–5 through to the end of the century. This allows the calculation of a wide range of climate exposure statistics aggregated by country or region, including hazard and difference values for a country/region weighted by either population or land area, as well as the exposed land area and population (either as a total or a percentage), and the comparison of these statistics for different SSPs. Exposure statistics are calculated for all ensemble members individually. Additionally, the mean as well as the 5th, 25th, 50th, 75th, and 95th percentile are assessed based on all ensemble members contributing to each GWL.

The ISIMIP fractional country mask at 0.5° spatial resolution (Perrette 2023) is used for calculating the statistics on a country-level basis. Additionally, the statistics are also assessed for the R10 regions (IPCC 2022a), the IPCC AR6-WGI reference regions (Iturbide *et al* 2020), the UN R5 regions (www.un.org/dgacm/en/content/regional-groups), and the EU27.

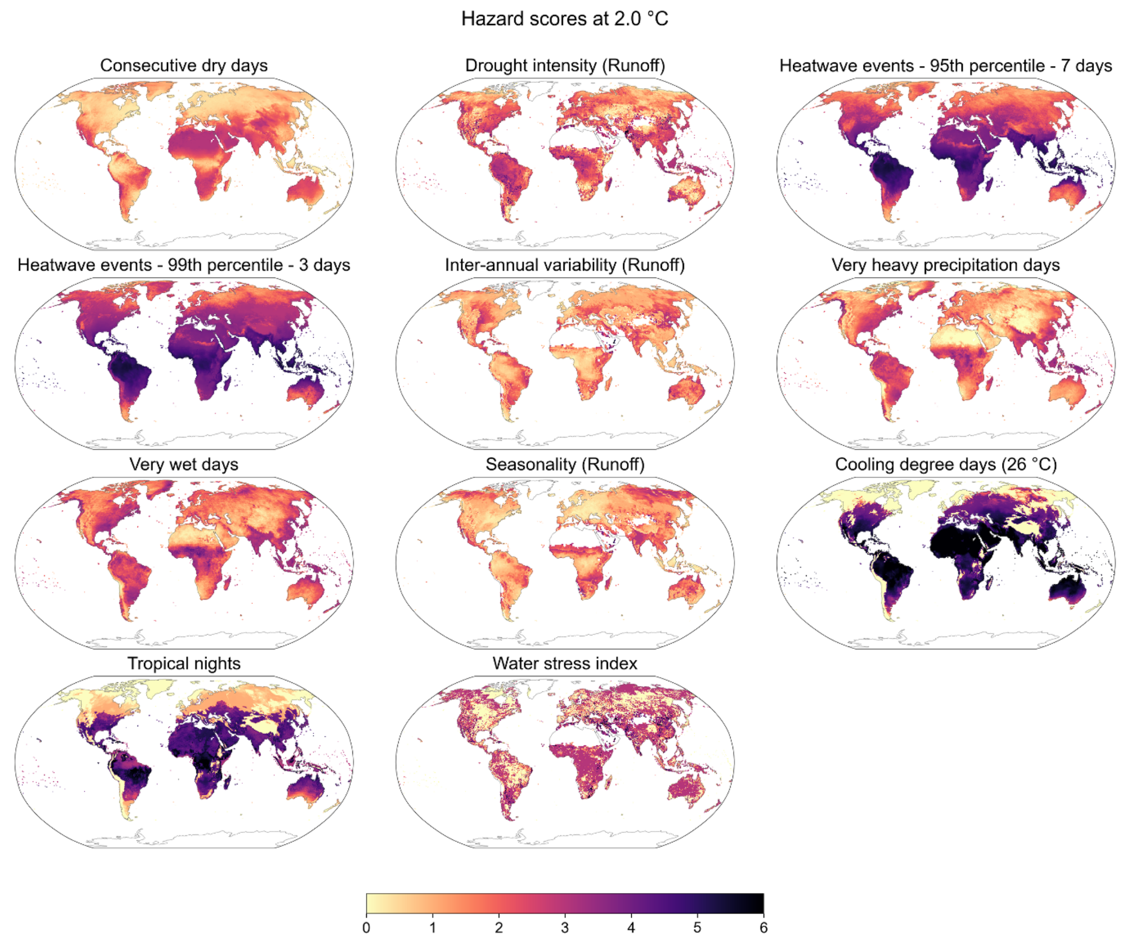

Figure 4. Hazard score at 2.0 °C for a selection of indicators. Desert areas and the Greenland ice sheet have been masked out for the hydrology indicators due to lack of confidence in the modelling results for these regions. Temperature-based indicators, such as 'Heatwave events' or 'Tropical nights' show comparatively higher scores than the precipitation or hydrology-based ones for all global warming levels due to the larger changes in air temperatures with increasing global mean temperature compared to other climatic input variables.

The exposure to climate hazards can be assessed at any hazard score level. For the table output published with our data, we included three different levels: land area and population exposed to at least low hazard (hazard score $\geqslant 1$), to at least medium hazard (hazard score $\geqslant 3$), and to high or very high hazard (hazard score $\geqslant 5$). The population or land area for grid cells that meet these criteria are summed for every country/region and divided by the entire land area or population per country/region.

3. Results and analysis

The climate change indicator dataset lends itself to a wide range of possible analyses. Focusing mainly on the data description in this paper, here we give an overview of the possibilities for data use. More in-depth analyses on certain themes is for further research, whilst the indicator maps together with national dashboards showing exposed populations can be explored in more detail on www.climate-solutions-explorer.eu.

3.1. Multi-hazard exposure

When assessing to how many indicators with at least medium hazard every grid cell is exposed to, this dataset shows that impacts manifest substantially even in the near term at lower GWLs (figure 5). For this analysis, a subset of 11 variants, considered to be a good representation of the indicator set, is selected. These variants are 'Consecutive dry days', 'Drought intensity (Runoff)', 'Heatwave events' (95th percentile/7 days representing less extreme, but longer events, and 99th percentile/3 days representing more extreme, but shorter events), 'Inter-annual variability (Runoff)', 'Very heavy precipitation days', 'Very wet days', 'Cooling degree days', 'Seasonality (Runoff)', 'Tropical nights', and 'Water stress index'.

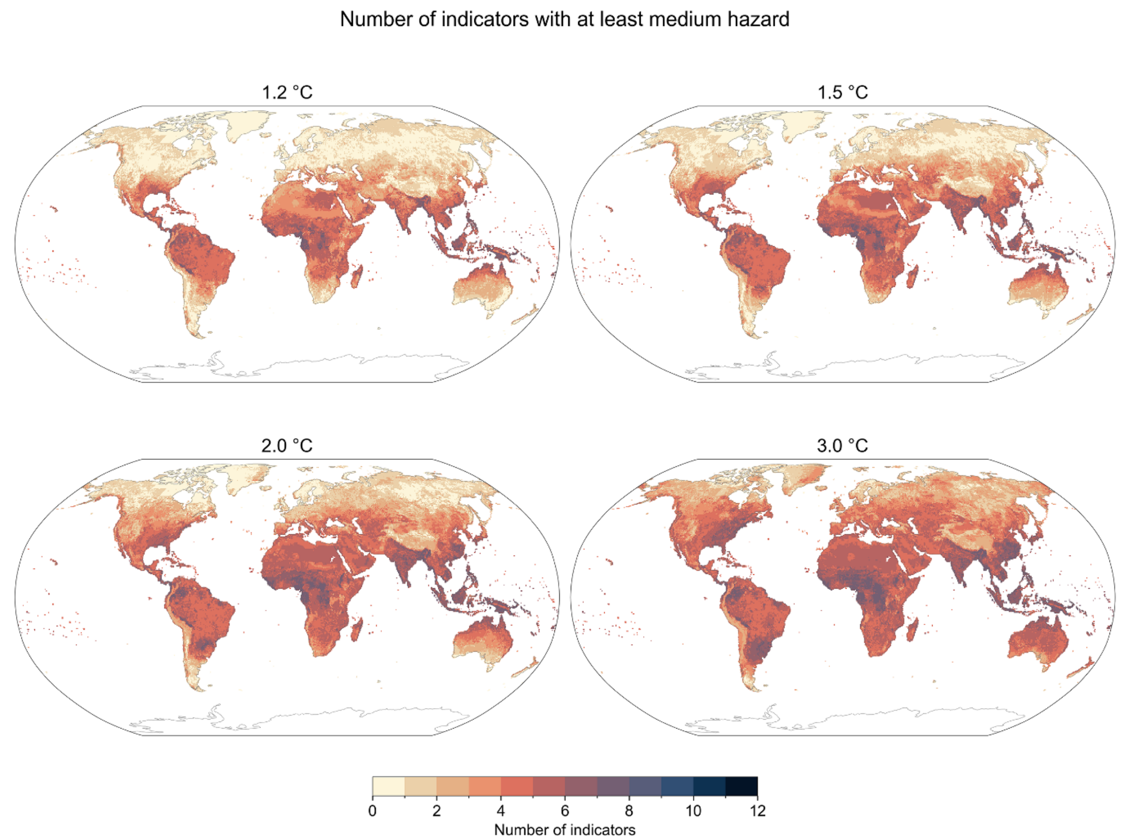

Figure 5. Number of indicators with at least medium hazard (hazard score ⩾ 3) for the global warming levels 1.2, 1.5, 2.0, and 3.0 °C. Even at 1.2 °C, large parts of the land area are already facing hazards from four or more indicators. With increasing global warming, the number of indicators increases, as well as the extent of the areas exposed to four or more indicators. At 3.0 °C, there are hardly any parts of the world that are not exposed to any hazards anymore. Note that due to the masking out of desert areas and the Greenland ice sheet for the hydrology indicators, the maximum number of indicators in these areas is lower.

At 1.5 °C, almost half of the global land area (46% using the multi-model median, with a range of 18%–65% for the 5th and 95th percentile across the multi-model range (figures SI 4–7)) is exposed to four or more indicators with at least medium hazard (figure 6). When considering the global population, about three-quarters (29%–91%) of the world's population are exposed to at least four indicators with at least medium hazard (using the population projections for SSP2 in the year 2050).

At high levels of global warming, exposure to higher numbers of indicators is expected. At a warming of 3.0 °C, there are very few areas which do not show a clear change in signal for any of the hazards, whereas most parts of the world would be exposed to at least medium hazard from four or more indicators (figure 5). Overall, areas in the low latitudes and the global south are more severely affected by multiple indicators, but even most of Europe, which is still relatively unaffected by medium or higher hazard scores below 2.0 °C compared to other parts of the world, faces at least medium hazard from three or more indicators at a warming of 3.0 °C. At this GWL, 1.3% (9%–0.05%) of the land area is exposed to zero additional hazards while almost 70% of the world (55%–85%) are impacted by four or more indicators; with 45% (23%–70%) exposed to at least five indicators (up from 26% (5%–52%) at 1.5 °C) and 5% (1%–21%) exposed to seven indicators. This amounts to 91% (78%–98%) of the world's population for at least four indicators (and 74% (40%–93%) and 14% (2%–52%) for at least five and seven indicators, respectively).

The high proportion of exposed population is more evident when including population density into the analysis (figure 7), as the land areas facing hazards from the highest number of indicators coincide with some of the most densely populated parts of the world. Low latitude and highly populated areas such as south Asia and central Africa are already highly exposed at 1.5 °C, whilst the number of indicators affecting populated areas in Europe, China, central Asia, and North America significantly increases the number of people exposed globally at subsequently higher GWLs.

Considering high hazards (figures SI 8 and 9), 65% (93%–49%) of the world's land area is not exposed to any indicators with high or very high hazards at 1.5 °C. A very similar picture presents itself for the world's population, with 61% (96%–29%) not affected. At 3.0 °C, this percentage reduces by one-third for the land

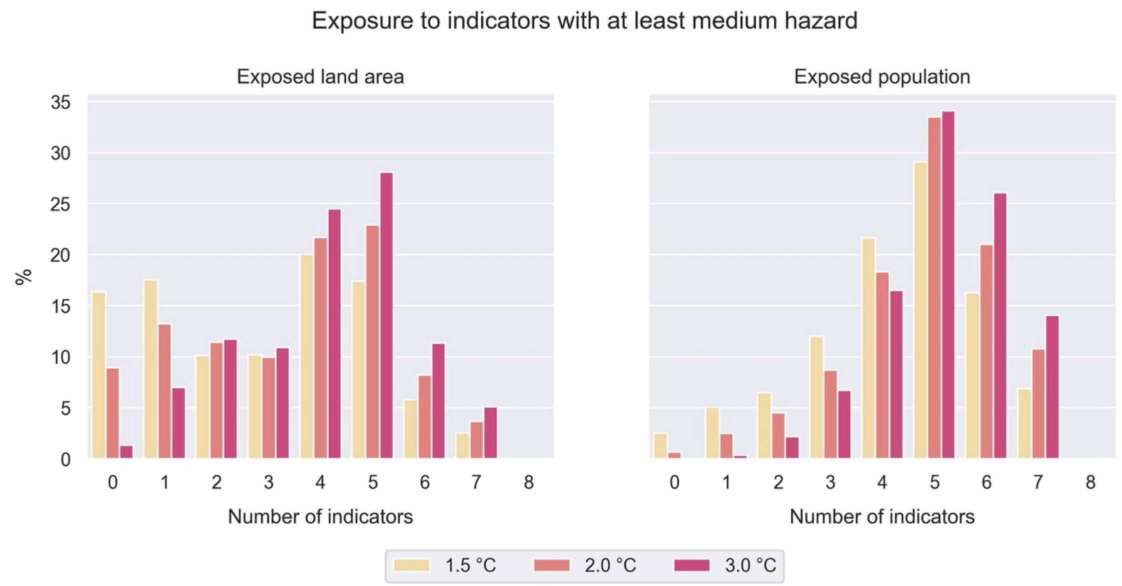

Figure 6. Exposure to indicators with at least medium hazard (hazard score ⩾ 3), for both land area (on the left) and population (on the right) using population projections for 2050 (SSP2). At a global warming level of 1.5 °C, just over half (56%) of the land area would be affected by three or more indicators with at least medium hazard, while only 16% of the land area are not exposed to any hazards. At 3.0 °C, almost half of the world's land surface (45%) is exposed to at least medium hazard from five or more indicators. At 1.5 °C, 86% of the world's population are exposed to at least three indicators with at least medium hazard. Higher global warming levels also increase the number of hazards that people are exposed to, and at 3.0 °C a similar amount of people (74% of the global population) are exposed to hazards from at least five indicators.

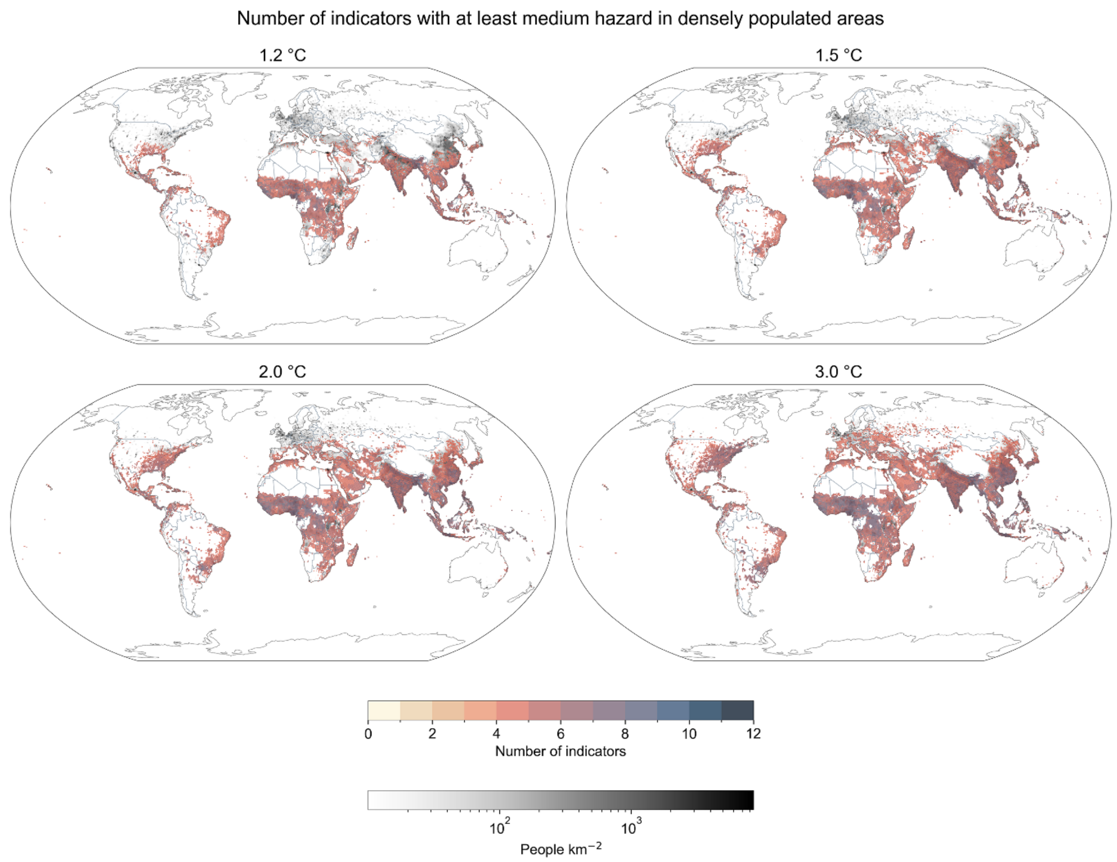

Figure 7. Map of densely populated areas (population density ⩾ 10 people km^{-2}, population projection from SSP2 in year 2050) overlain with the number of indicators (⩾4 indicators) with at least medium hazard (hazard score ⩾ 3). Areas with a high population density coincide with areas that are exposed to a high number of indicators, explaining why a higher percentage of population is affected compared to land area for all global warming levels.

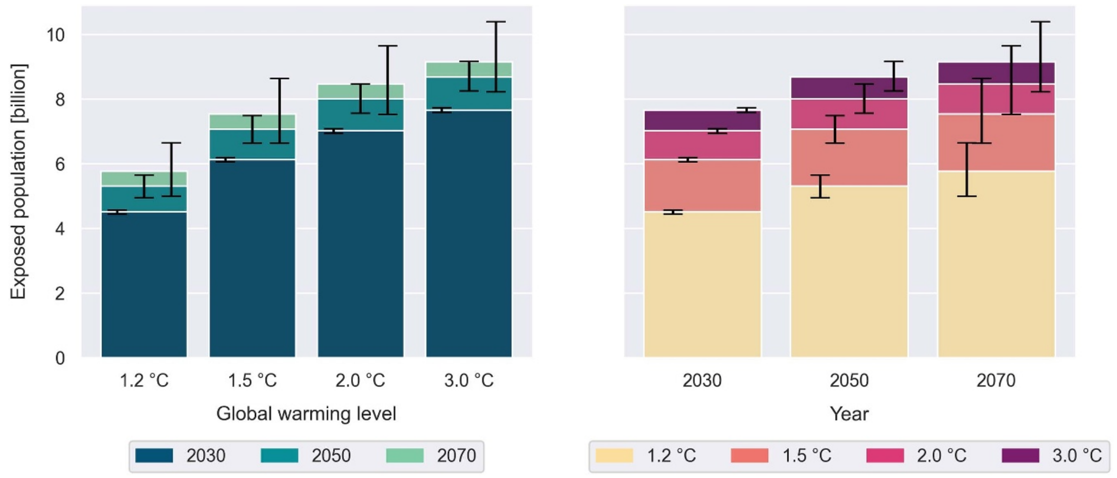

Figure 8. Exposed population to at least four indicators with at least medium hazard, shown for the global warming levels of 1.2 °C, 1.5 °C, 2.0 °C, and 3.0 °C, comparing the populations projected at different points in time, shown in this case for the middle of the road SSP2 projections. The black bars show the possible range in exposed population across the other available population projections (SSP1, SSP3, SSP4, and SSP5). Whilst 3.0 °C warming in 2030 is considered to be a highly unlikely outcome, it is necessarily shown here to illustrate the incremental exposure at later time slices.

surface area to 44% (49%–37%) and by 2/3 to 23% (33%–15%) for the population. Inversely, the land area exposed to at least two indicators with at least high hazard rises from ca. 9% (1%–24%) at 1.5 °C to 43% (26%–50%) at 3.0 °C and from 10% (0.3%–32%) to 60% (30%–75%) for the exposed population. While the hazards are again predominantly limited to Sub-Saharan Africa, the tropics, and South–East Asia, parts of North America and Europe are also facing exposure to severe hazards at a warming of 2.0 °C and above.

At the lower end of the hazard score range, large parts of the world's land surface and population will be affected by hazards from multiple indicators with at least low impact (figures SI 10 and 11). While the impact of each indicator on its own might not be very severe, the compounding effects could put a high strain on societies and ecosystems.

3.2. Effect of population on multi-hazard exposure

The total exposed population does not only depend on the GWL, but also on the year at which that GWL is reached and the population expected at the time. As the population projections for all five SSPs considered here project rising populations until at least the middle of the century, the potential population exposure to climate impacts thus increases not only with higher GWL, but also with time, depending on the SSP. Additionally, the number of people exposed is considerably smaller for SSP1 and SSP5 (lower end of the black bar), in which increased investments in education and health lead to relatively lower population projections, whereas significantly more people are exposed for SSP3 due a high population growth in developing countries (figure 8).

3.3. Regional population exposure to key hazards

The provided table output data also facilitate the analysis of different indicators by country or region (figure 9). In line with earlier observations on the higher hazard scores for temperature-based indicators, 'Heatwave events' shows some of the highest percentages of exposed population to at least medium hazard. For regions where a high percentage of population is already exposed at a lower GWL of 1.5 °C, the number of exposed people does not change much with increasing warming. However, a significant increase in exposed population between 1.5 °C and 3.0 °C can be observed for the EU and North America, where the total population that is exposed rises from 12% (0.4%–27%) to 81% (48%–96%), and from 42% (3%–64%) to 94% (89%–97%), respectively. For 'Water stress index', the number of exposed people stays relatively constant between 1.5 °C and 3.0 °C in all regions, with the levels in exposure only rising by a few percent between each GWL as socioeconomic demands for water are the dominant driver for this indicator When it comes to the precipitation-based indicator 'Very wet days', the picture looks more mixed. While some areas that are already facing high amounts of precipitation today, such as Southern Asia, are not facing a big change with increasing warming, the exposed population in other areas, such as North America, almost doubles between 1.5 °C and 3.0 °C.

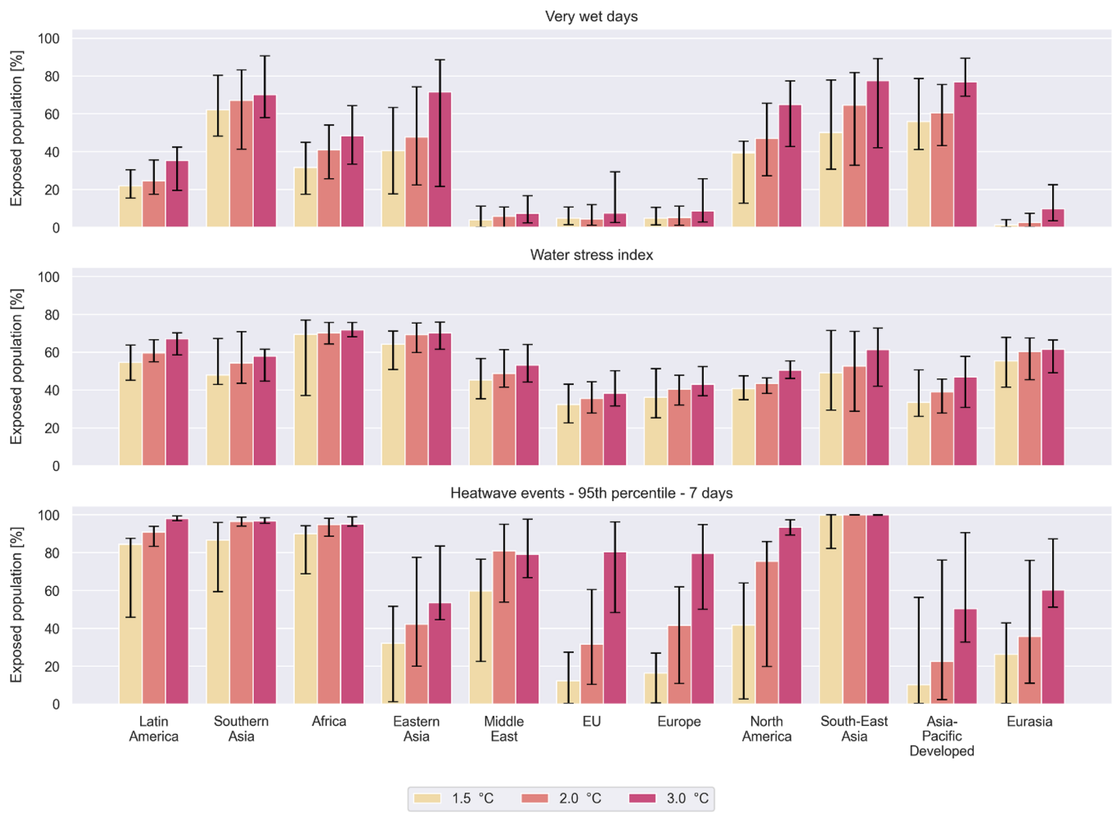

Figure 9. Exposed population to at least medium hazard for the indicators 'Very wet days', 'Water stress index', and 'Heatwave events—95th percentile—7 days', shown for three global warming levels and the R10 regions as well as the EU using the population projection from SSP2 in year 2050. The error bars show the uncertainty range spanned by all available ensemble members.

4. Discussion

Arriving at the datasets presented is the result of various iterations in methods, assumptions, and exploration of uncertainties. A primary methodological concern was to develop a hazard score which appropriately considers both the absolute values and the relative changes experienced at different GWLs, thereby advancing the method used by Byers *et al* (2018), who transformed indicators onto a common risk scale by applying score ranges, which were defined by the interrogation of the original data, expert judgement and sensitivity analysis, but only considered either the change in value or the absolute value. Our method for the score conversion presented here still has the possibility to easily include expert judgement in the process (as done for the water stress indicator for example), but the approach can also be applied to a broad range of indicators for which agreement on what constitutes a hazard is lacking or depends on the region of interest.

One important consideration for this type of analysis is the impact of uncertainty on the results. The climate model uncertainty explored through the five GCMs indicates that there could be significant differences in exposure for most regions, depending on the indicator (figure 9). Whilst the five GCMs used in ISIMIP are selected to largely cover the ranges in the CMIP6 ensemble, it is nonetheless possible that impacts are experienced outside of these ranges. As the intended target group for this dataset also includes audiences with a less scientific background, the choice was made to use the multi-model median for the main outputs for ease of use. We do, however, also provide the results for all available ensemble member, allowing a more knowledgeable audience to explore the uncertainty space spanned by the five GCMs in more detail. Whilst it must be acknowledged that there is a certain cascading of uncertainty along the assessment chain (Wilby and Dessai 2010), the previous assessment (Byers *et al* 2018) also showed that the main driver of uncertainty in terms of exposure and vulnerability is driven by socioeconomic uncertainties in population numbers and distribution, as well as their relative vulnerability levels, which in coming decades could be an order of magnitude different depending on changes in income and inequality.

Another key factor not incorporated due to the GWL approach is the speed of change, which, for ecosystems and for societal response alike, affects the impact experienced if there is less time for adaptation and building resilience (Schleussner *et al* 2021). While slower warming gives more time to adapt and the population on average might therefore be less vulnerable (e.g. due to an increase in wealth or adaptive capacity), this effect could be outweighed by the overall increase in population, which is most likely to occur in places where vulnerability is already at its highest. Warming will continue at least until carbon dioxide emissions are net zero; expected in the 2050s in the best case scenario (Riahi *et al* 2022, IPCC 2022b), with >30% chance that localized warming and extremes are still experienced in the decade post net-zero (Diffenbaugh *et al* 2023). With higher populations of SSP2, SSP3, and SSP4, the differences in exposure due to population growth grow later in the century and are as large as the differences in GWLs (figure 8). An important caveat of these exposure estimates is the absence of adaptation (Andrijevic *et al* 2023), therefore these figures should be considered upper bounds on exposure for each SSP.

Finding a conversion to a hazard score that yields good results for different types of indicators depends on several factors, in particular the choice of reference period, and subsequently the change that occurs between the reference period and the assessed GWLs. Whilst not assessed here, different reference periods to the one used (1974–2004) would yield different results, but crucially depend on consistent data availability across the ensemble of model runs. The hazard posed by an indicator is also influenced by the baseline condition of the reference period. Places with already extreme conditions generally experience relatively small changes, whilst places with more moderate conditions can be expected to experience larger changes. This bivariate approach is designed to capture these nuances by attributing scores based on the relative change but modulated by the absolute conditions. A significant increase in hazard in a place that hasn't faced any hazard before might have severe consequences due to a lack of preparation for, or familiarity with, these kinds of hazards and extremes. While it is difficult to exactly attribute an accurate hazard score to these situations, the absolute component of our bivariate score can at least partly capture the risk.

A final caveat for developing a hazard score is the fact that some indicators are more context specific to the land climate dynamics, such as hydrology. To reflect these differences, the Köppen–Geiger climate zones were used to group the absolute values of the reference period before calculating the percentiles for certain hydrology indicators. The hard boundaries between zones in the dataset, which do not necessarily occur in reality, introduce some slightly abrupt changes in score values on the maps, but overall much improve the distribution of scores. Future work could investigate potentially smoothing these hard edges between climate zones.

In terms of the interpretation of the dataset, certain types of analyses demand nuanced considerations from the user. For analysing multi-hazard exposure from a selection of indicators, caution needs to be exercised to avoid double-counting of indicators that are closely related and thus likely highly correlated (figure SI 12), such as 'Wet days' and 'Very wet days', or the different variants of 'Heatwave events'. Additionally, the smaller range of available GWLs for the hydrology indicators and the fact that the Greenland ice sheet and the desert areas have been masked out should be taken into consideration for these types of analyses. It should also be noted that whilst this dataset offers the option to explore spatially compounding hazards, temporally compounding hazards cannot be captured due to our chosen methods, and this dataset, therefore, cannot serve the needs of analyses requiring this type of information.

Furthermore, using this database for detailed analysis at the grid cell level and for the analysis of very small countries should be done with caution due to the limitations of the GCMs in modelling smaller-scale processes. Analyses at the global and regional scale as well as comparative analyses between GWLs and SSPs can, however, provide valuable insights. It should still be noted that the aggregation of the data to the national or regional level smooths out existing heterogeneities within countries or regions.

Overall, the bivariate approach developed and applied to this indicator set provides an improved approximation over previous similar assessments, and sets a foundation for more comprehensive, globally consistent climate risk assessment, when combined with exposure and vulnerability datasets. This could include, for example, incorporating demographic and socioeconomic data such as age cohorts (Thiery *et al* 2021) or income levels (Byers *et al* 2018, Doan *et al* 2023), and access to technological adaptation such as access to cooling to alleviate heat stress (Andrijevic *et al* 2021, Mastrucci *et al* 2021). Combining the dataset with data on the limits to water- (Lissner *et al* 2024) and irrigation-related adaptation (Maanen *et al* 2022), as well as with data on the respective institutional, sectoral, and individual capacities to adapt (Andrijevic *et al* 2023) could not only add another dimension to the data anlysis, but could also strengthen its applicability for adaption-planning purposes.

5. Conclusions

As the number of climate change impacts steadily grows around the globe due to a rise in GMT, there is urgent need to assess where people will be affected most by multiple risks. Comparing the risks posed by different hazards is challenging, especially for non-experts who are lacking the ability to make the necessary judgements. This new, publicly available database contains insights on climate hazards from CMIP global climate models, removing computational constraints and making this type of data more accessible to non-experts due to its compact size and provided visualisations (www.climate-solutions-explorer.eu). Furthermore, the score metric simplifies the process of comparing the risks posed by different indicators to each other.

The database can be used for a variety of analyses. For example, indicators can be examined individually at the regional or national level, which shows that the population exposed to at least medium hazard from the indicator 'Heatwave events' in the EU increases from 12% to 80% between 1.5 °C and 3.0 °C (figure 9). Furthermore, a multi-hazard analysis using 11 different indicators reveals that mitigating to 1.5 °C could avoid a doubling in the number of people exposed to a high or very high hazard from any of these indicators (figure SI 9). The database can also serve as the starting point for further research, such as emulating climate impacts from IAM scenarios (Byers *et al* 2024) or identifying climate impact vulnerability hotspots (Werning and Byers *et al* 2024).

With the development of further ISIMIP datasets, additional indicators could easily be added in the future, making this database even more versatile. At a point in time when the window for reducing the risk burden is rapidly closing, it is crucial to understand how global climate impacts are changing to inform adaptation action. The easily accessible and digestible database can disseminate the required knowledge that stakeholders, practitioners, and the general public need for this.

Data availability statement

The data that support the findings of this study are openly available at the following URL/DOI: https://zenodo.org/doi/10.5281/zenodo.13753537 (v1.0) (Werning and Frank *et al* 2024). The dataset includes:

- Global gridded projections of the multi-model median in netCDF format of all climate change indicators at 0.5° spatial resolution and for the global warming levels of 1.2 °C, 1.5 °C, 2.0 °C, 2.5 °C, 3.0 °C, and 3.5 °C

  Indicators are grouped by category and provided as .zip files. The indicator 'Cooling degree days' is included in energy.zip as the grouping of the indicators for the .zip files was done in line with the indicator categories used for the Climate Solutions Explorer website. For each GWL, maps for the absolute indicator values, the relative difference, and the scores are provided. The naming format is: cse_[short_indicator_name]_[ssp]_[gwl]_[metric].nc4. Please note that the Greenland ice sheet and the desert areas have been masked out for the hydrology indicators for these datasets.

- Intermediate output data, including gridded maps of absolute values, relative differences, and scores for all ensemble members, as well as gridded maps of the multi-model ensemble statistics for the GWLs and the reference period

  For the ensemble member data, the naming format is [gcm]_[ssp/rcp]_[gwl]_[short_indicator_name]_global_[start_year]_[end_year].nc4 or [ghm]_[gcm]_[ssp/rcp]_[gwl]_[soc]_[short_indicator_name]_global_[start_year]_[end_year]_[metric].nc4 for the hydrology indicators.

- Tabular data (.csv) aggregating the indicators to country or region level, for both hazards and exposure, population and land-area weighted

  The .zip archives 'table_output_climate_exposure_{aggregation_level}.zip' contain the tabular data for all indicators. Four different aggregation levels are provided: country level, R10 regions and the EU, IPCC AR6-WGI reference regions, and UN R5 regions.

The dataset also includes additional indicators (e.g. air pollution) that were created for the Climate Solutions Explorer website, but are not part of the indicator selection presented here.

The spatial maps of the indicators can be explored in more detail on www.climate-solutions-explorer.eu in the 'Impacts Explorer'. The 'Impacts' page under 'National Dashboards' shows the exposure data and avoided impacts for key risks for different countries and regions.

The population data used for the exposure calculations is publicly available and can be downloaded from https://zenodo.org/doi/10.5281/zenodo.13745063 (Werning 2024).

The code that was used to generate the data is available on GitHub (https://github.com/iiasa/cse_impact_data). The scientific colour maps created by Fabio Crameri were used in some of the plots (Crameri 2023).

Acknowledgment

We acknowledge the European Union's Horizon 2020 research and innovation program for funding the development of this research as part of the ENGAGE project (Grant Agreement #821471). The Climate Solutions Explorer builds on the Global Hotspots Explorer, which was funded by Global Environment Facility under contract #6993—the support in development and maintenance of these tools by the IIASA Scenario Services team, in particular Maximilian Wolschlager, is gratefully acknowledged. We also acknowledge ISIMIP and its community and would especially like to thank Katja Frieler, Stefan Lange, Wim Thiery, and Yusuke Satoh for their support on various aspects. Additionally, we would like to acknowledge the continued national member organization support of IIASA and thank all our colleagues at IIASA who have contributed to the creation of this dataset with their knowledge, advice, and support.

Conflict of interest

The contact author has declared that none of the authors has any competing interests.

Financial support

This research has been supported by the European Union's Horizon 2020 research and innovation program under Grant Agreement No. 821471 (ENGAGE).

Author contributions

M W processed the data for all indicators and wrote the code. D H assisted with the data processing. M W, E B, and D H developed the method for the bivariate score. The manuscript was written jointly by M W and E B with contributions from D H, V K, K R and BvR. M W and D H produced the figures and tables. Conceptualization and coordination of the study was done by E B, V K, K R and BvR.

ORCID iDs

Michaela Werning https://orcid.org/0000-0002-8684-9608
Daniel Hooke https://orcid.org/0009-0000-6403-4275
Volker Krey https://orcid.org/0000-0003-0307-3515
Keywan Riahi https://orcid.org/0000-0001-7193-3498
Bas van Ruijven https://orcid.org/0000-0003-1232-5892
Edward A Byers https://orcid.org/0000-0003-0349-5742

References

Allen M R *et al* 2018 Framing and Contex *Global Warming of 1.5 °C. An IPCC Special Report on the Impacts of Global Warming of 1.5 °C above Pre-industrial Levels and Related Global Greenhouse Gas Emission Pathways, in the Context of Strengthening the Global Response to the Threat of Climate Change, Sustainable Development, and Efforts to Eradicate Poverty* 1st edn, ed V Masson-Delmotte *et al* (Cambridge University Press) pp 49–92

Andrijevic M, Byers E, Mastrucci A, Smits J and Fuss S 2021 Future cooling gap in shared socioeconomic pathways *Environ. Res. Lett.* **16** 094053

Andrijevic M, Schleussner C-F, Crespo Cuaresma J, Lissner T, Muttarak R, Riahi K, Theokritoff E, Thomas A, van Maanen N and Byers E 2023 Towards scenario representation of adaptive capacity for global climate change assessments *Nat. Clim. Change* **13** 778–87

Beck H E, Zimmermann N E, McVicar T R, Vergopolan N, Berg A and Wood E F 2018 Present and future Köppen-Geiger climate classification maps at 1-km resolution Sci Data **5**

Burek P *et al* 2016 *Water Futures and Solution—Fast Track Initiative (Final Report)* (IIASA) WP-16-006 (available at: https://iiasa.dev.local/) (Accessed 8 May 2024)

Byers E A *et al* 2024 First applications of the rapid impact model emulator *Copernicus Meetings* EGU24-12642 (https://doi.org/10.5194/egusphere-egu24-12642)

Byers E *et al* 2018 Global exposure and vulnerability to multi-sector development and climate change hotspots *Environ. Res. Lett.* **13** 055012

Climate Analytics 2022 Climate impact explorer (available at: http://climate-impact-explorer.climateanalytics.org/)

Crameri Fabian Scientific colour maps (8.0.1) 2023 Zenodo (https://doi.org/10.5281/zenodo.8409685)

Diffenbaugh N S, Barnes E A and Keys P W 2023 Probability of continued local-scale warming and extreme events during and after decarbonization *Environ. Res. Clim.* **2** 021003

Diffenbaugh N S and Giorgi F 2012 Climate change hotspots in the CMIP5 global climate model ensemble *Clim. Change* **114** 813–22

Diffenbaugh N S, Giorgi F, Raymond L and Bi X 2007 Indicators of 21st century socioclimatic exposure *Proc. Natl Acad. Sci.* **104** 20195–8

Doan M K *et al* 2023 *Counting People Exposed to, Vulnerable to, or at High Risk from Climate Shocks: A Methodology* (World Bank) (https://doi.org/10.1596/1813-9450-10619)

EEA 2022 European climate data explorer intro—english (available at: https://climate-adapt.eea.europa.eu/en/knowledge/european-climate-data-explorer/)

Field C B *et al* (eds) 2012 Managing the risks of extreme events and disasters to advance climate change adaptation—IPCC *The Edinburgh Building, Shaftesbury Road, Cambridge CB2 8RU ENGLAND* (Cambridge University Press) p 582 (available at: www.ipcc.ch/report/managing-the-risks-of-extreme-events-and-disasters-to-advance-climate-change-adaptation/) (Accessed 8 May 2024)

Forster P M *et al* 2024 Indicators of global climate change 2023: annual update of key indicators of the state of the climate system and human influence *Earth Syst. Sci. Data* **16** 2625–58

Frieler K *et al* 2017 Assessing the impacts of 1.5 C global warming–simulation protocol of the inter-sectoral impact model intercomparison project (ISIMIP2b) *Geosci. Model Dev.* **10** 4321–45

Frieler K *et al* 2024a Scenario setup and forcing data for impact model evaluation and impact attribution within the third round of the inter-sectoral impact model intercomparison project (ISIMIP3a) *Geosci. Model Dev.* **17** 1–51

Frieler K *et al* 2024b Scenario set-up and the new CMIP6-based climate-related forcings provided within the third round of the inter-sectoral intercomparison project (ISIMIP3b, group I and II) *Geosci. Model Dev.* submitted

Giorgi F 2006 Climate change hot-spots *Geophys. Res. Lett.* **33** L08707

Gosling S N *et al* 2023 *ISIMIP2b Simulation Data from the Global Water Sector* (ISIMIP Repository) (https://doi.org/10.48364/ISIMIP.626689)

Hanasaki N, Yoshikawa S, Pokhrel Y and Kanae S 2018 A global hydrological simulation to specify the sources of water used by humans *Hydrol. Earth Syst. Sci.* **22** 789–817

IIASA 2019 *Global Hotspots Explorer* (available at: https://hotspots-explorer.org/)

IPCC 2022a Annex II: definitions, units and conventions *Climate Change 2022: Mitigation of Climate Change. Contribution of Working Group III to the Sixth Assessment Report of the Intergovernmental Panel on Climate Change* 1st edn ed A Al Khourdaje *et al* (Cambridge University Press) pp 1821–40

IPCC (ed) 2022b *Climate Change 2022—Mitigation of Climate Change: Working Group III Contribution to the Sixth Assessment Report of the Intergovernmental Panel on Climate Change* 1st edn (Cambridge University Press) (https://doi.org/10.1017/9781009157926)

IPCC 2022c IPCC AR6-WGI Atlas (available at: https://interactive-atlas.ipcc.ch/atlas)

ISIMIP 2022 ISIpedia (available at: www.isipedia.org/)

Iturbide M *et al* 2020 An update of IPCC climate reference regions for subcontinental analysis of climate model data: definition and aggregated datasets *Earth Syst. Sci. Data* **12** 2959–70

James R, Washington R, Schleussner C-F, Rogelj J and Conway D 2017 Characterizing half-a-degree difference: a review of methods for identifying regional climate responses to global warming targets *WIREs Clim. Change* **8** e457

Jones B and O'Neill B C 2016 Spatially explicit global population scenarios consistent with the shared socioeconomic pathways *Environ. Res. Lett.* **11** 084003

Kc S and Lutz W 2017 The human core of the shared socioeconomic pathways: population scenarios by age, sex and level of education for all countries to 2100′ *Glob. Environ. Change* **42** 181–92

KC S, Potancokova M, Adhikari S, Yildiz D, Mamolo M, Sobotka T, Zeman K, Abel G, Lutz W and Goujon A Wittgenstein Center (WIC) Population and Human Capital Projections - 2023 (Version V13) 2024 Zenodo (https://doi.org/10.5281/zenodo.10618931)

Klein Tank A M G, Zwiers F W and Zhang X 2009 *Guidelines on Analysis of Extremes in a Changing Climate in Support of Informed Decisions for Adaptation* (WMO)

Lange S 2019 Trend-preserving bias adjustment and statistical downscaling with ISIMIP3BASD (v1.0) *Geosci. Model Dev.* **12** 3055–70

Lange S *et al* 2020 Projecting exposure to extreme climate impact events across six event categories and three spatial scales *Earth's Future* **8** e2020EF001616

Lange S 2021 *ISIMIP3b Bias Adjustment Fact Sheet* (available at: www.isimip.org/documents/413/ISIMIP3b_bias_adjustment_fact_sheet_Gnsz7CO.pdf) (Accessed 5 February 2024)

Lange S and Büchner M 2017 *ISIMIP2b Bias-Adjusted Atmospheric Climate Input Data* (ISIMIP Repository) (https://doi.org/10.48364/ISIMIP.208515)

Lange S and Büchner M 2021 *ISIMIP3b Bias-Adjusted Atmospheric Climate Input Data* (ISIMIP Repository) (https://doi.org/10.48364/ISIMIP.842396.1)

Lissner T K, Möller T, Caretta M A and Mukherji A 2024 Effectiveness of water-related adaptation decreases with increasing warming *One Earth* **7** 444–54

Maanen N V, Andrijevic M, Lejeune Q, Rosa L, Lissner T and Schleussner C-F 2022 Accounting for socioeconomic constraints in sustainable irrigation expansion assessments *Environ. Res. Lett.* **17** 075004

Mastrucci A, van Ruijven B, Byers E, Poblete-Cazenave M and Pachauri S 2021 Global scenarios of residential heating and cooling energy demand and CO_2 emissions *Clim. Change* **168** 14

O'Neill B C *et al* 2017 The roads ahead: Narratives for shared socioeconomic pathways describing world futures in the 21st century *Global Environmental Change* **42** 169–80

Perrette M 2023 ISI-MIP/isipedia-countries (v2.6) (available at: https://github.com/ISI-MIP/isipedia-countries/releases/tag/v2.6)

Piontek F *et al* 2014 Multisectoral climate impact hotspots in a warming world *Proc. Natl Acad. Sci.* **111** 3233–8

Raskin P 1997 *Water Futures: Assessment of Long-range Patterns and Problems* (WMO) p 92

Riahi K *et al* 2017 The shared socioeconomic pathways and their energy, land use, and greenhouse gas emissions implications: an overview *Glob. Environ. Change* **42** 153–68

Riahi K *et al* 2022 Mitigation pathways compatible with long-term goals *IPCC 2022: Climate Change 2022: Mitigation of Climate Change: Working Group III Contribution to the Sixth Assessment Report of the Intergovernmental Panel on Climate Change* (Cambridge University Press) pp 295–408

Rising J, Tedesco M, Piontek F and Stainforth D A 2022 The missing risks of climate change *Nature* **610** 643–51

Satoh Y *et al* 2017 Multi-model and multi-scenario assessments of Asian water futures: the water futures and solutions (WFaS) initiative *Earth's Future* **5** 823–52

Schleussner C-F *et al* 2016 Differential climate impacts for policy-relevant limits to global warming: the case of 1.5 °C and 2 °C *Earth Syst. Dyn.* **7** 327–51

Schleussner C-F, Pfleiderer P, Andrijevic M, Vogel M M, Otto F E L and Seneviratne S I 2021 Pathways of climate resilience over the 21st century *Environ. Res. Lett.* **16** 054058

Schurer A P, Mann M E, Hawkins E, Tett S F B and Hegerl G C 2017 Importance of the pre-industrial baseline for likelihood of exceeding Paris goals *Nat. Clim. Change* **7** 563–7

Sun Q, Miao C, Hanel M, Borthwick A G L, Duan Q, Ji D and Li H 2019 Global heat stress on health, wildfires, and agricultural crops under different levels of climate warming *Environ. Int.* **128** 125–36

Takata K, Emori S and Watanabe T 2003 Development of the minimal advanced treatments of surface interaction and runoff *Glob. Planet. Change* **38** 209–22

Thiery W *et al* 2021 Intergenerational inequities in exposure to climate extremes *Science* **374** 158–60

von Bloh W, Schaphoff S, Müller C, Rolinski S, Waha K and Zaehle S 2018 Implementing the nitrogen cycle into the dynamic global vegetation, hydrology, and crop growth model LPJmL (version 5.0) *Geosci. Model Dev.* **11** 2789–812

Wanders N and Wada Y 2015 Human and climate impacts on the 21st century hydrological drought *J. Hydrol.* **526** 208–20

Werning M *et al* 2024 Climate solutions explorer—hazard, impacts and exposure data, v1.0′ *Zenodo* (https://doi.org/10.5281/zenodo.13753537)

Werning M 2024 Gridded maps of global population scaled to match the 2023 Wittgenstein center (WIC) population projections *Zenodo* (https://doi.org/10.5281/zenodo.13745063)

Werning M, Byers E, Hooke D, Andrijevic M, Krey V and Riahi K 2024 Comprehensive assessment of hazard, exposure, and vulnerability using a new database of climate impact indicators to identify hotspots for adaptation needs *Copernicus Meetings* EGU24-17789 (https://doi.org/10.5194/egusphere-egu24-17789)

Wilby R L and Dessai S 2010 Robust adaptation to climate change *Weather* **65** 180–5

Williams J W, Jackson S T and Kutzbach J E 2007 Projected distributions of novel and disappearing climates by 2100 AD *Proc. Natl Acad. Sci.* **104** 5738–42

World Bank 2021 Climate change knowledge portal (available at: https://climateknowledgeportal.worldbank.org/)